Journal of Gerontology: BIOLOGICAL SCIENCES
2008, Vol. 63A, No. 3, 219–231

Cells From Long-Lived Mutant Mice Exhibit Enhanced Repair of Ultraviolet Lesions

Adam B. Salmon,[1] Mats Ljungman,[1,2] and Richard A. Miller[1,3]

[1]Cellular and Molecular Biology Graduate Program, and [2]Department of Radiation Oncology, Division of Radiation & Cancer Biology, University of Michigan Comprehensive Cancer Center, University of Michigan Medical School, Ann Arbor. [3]Department of Pathology, Geriatrics Center, and VA Medical Center, University of Michigan, Ann Arbor.

Fibroblasts isolated from long-lived hypopituitary dwarf mice are resistant to many cell stresses, including ultraviolet (UV) light and methyl methane sulfonate (MMS), which induce cell death by producing DNA damage. Here we report that cells from Snell dwarf mice recover more rapidly than controls from the inhibition of RNA synthesis induced by UV damage. Recovery of messenger RNA (mRNA) synthesis in particular is more rapid in dwarf cells, suggesting enhanced repair of the actively transcribing genes in dwarf-derived cells. At early time points, there was no difference in the repair of cyclobutane pyrimidine dimers (CPD) or 6-4 photoproducts (6-4PP) in the whole genome, nor was there any significant difference in the repair of UV lesions in specific genes. However, at later time points we found that more lesions had been removed from the genome of dwarf-derived cells. We have also found that cells from dwarf mice express higher levels of the nucleotide excision repair proteins XPC and CSA, suggesting a causal link to enhanced DNA repair. Overall, these data suggest a mechanism for the UV resistance of Snell dwarf-derived fibroblasts that could contribute to the delay of aging and neoplasia in these mice.

Key Words: Longevity—Nucleotide excision repair—Snell dwarf—Stress resistance—Ultraviolet light.

LITTLE is understood of the cellular mechanisms that lead to the gradual physical decline and increased susceptibility to disease that are associated with the aging process in mammals. Mutant mice with extended life spans may provide valuable resources for these studies. Snell dwarf mice have a homozygous loss-of-function mutation of the *Pit1* gene, which encodes a transcription factor regulating anterior pituitary development (1). Snell dwarf mice therefore have nearly undetectable, circulating levels of growth hormone (GH) and its mediator insulin-like growth factor I (IGF-I), thyroid-stimulating hormone, and prolactin (2). These changes in the hormonal profile reduce young adult size by about 70%, extend life span approximately 40% (3), and lead to delays in many forms of pathology associated with the aging process, including arthritis, collagen cross-linking, T-cell subset changes, and the development of cataracts and glomerular lesions (3–5). These mice, as well as the phenotypically similar Ames dwarf mutants, also show a delay in the occurrence of spontaneous cancer and tend to die from cancer at a diminished rate compared to littermate controls (5,6).

Mechanisms that regulate aging may overlap with those that regulate cellular resistance to stress. Single-gene mutations that lead to an extension of life span in *Caenorhabditis elegans* tend to render those worms resistant to death induced by oxidative and nonoxidative stressors (7). To some extent, these results have been recapitulated in *Drosophila* and the mouse (8–10). For example, we have previously found that three mutations that increase life span and diminish serum IGF-I, the Ames and Snell dwarf mutations and a growth hormone receptor knockout mutation, render cells derived from these animals resistant to agents that induce cellular stress. Fibroblasts derived from Snell dwarf mice are resistant to the lethal effects of a variety of toxic agents, including oxidizing agents like paraquat and hydrogen peroxide, the heavy metal cadmium, DNA damaging agents such as ultraviolet (UV) light and methyl methanesulfonate (MMS), and incubation at 42°C (11,12). Fibroblasts from Ames dwarf mice were also shown to be resistant to paraquat, peroxide, cadmium, and UV light relative to control, and fibroblasts derived from GH receptor knockout mice were resistant to paraquat, peroxide, and UV light (12). We have shown that resistance to these agents is regulated by both oxidative stress-dependent and -independent pathways (12). In addition, these cells are resistant to the nonlethal metabolic effects of low-glucose medium and to the mitochondrial inhibitor rotenone (13). Snell dwarf cells are also relatively resistant to growth inhibition produced by long-term culture in 20% oxygen (14).

There is increasing interest in the role of DNA damage and repair in the regulation of aging and the progression of age-related disease, particularly the development of cancer (15,16). The response to DNA damage may also be important in the regulation of cellular stress resistance of Snell dwarf mice. In particular, they are resistant to cell

death induced by UV-C light and by MMS, agents that are lethal primarily because of the lesions they induce in the cell's genome. The relationship between the formation and repair of genomic lesions and the pathways that lead to cell death are well understood. The genomic adducts formed by the energy of UV light inhibit progression of the polymerases responsible for DNA replication and transcription; these lesions lead to cell cycle arrest and apoptosis if left unrepaired (17–22). UV lesions are primarily removed by nucleotide excision repair (NER), which includes both global genome repair (GGR) of lesions in the whole genome, as well as transcription-coupled repair (TCR) of lesions located in transcribed, protein-encoding genes. Cells with deficient TCR are particularly sensitive to the effects of UV radiation and undergo apoptosis at relative low doses of UV light (23). In addition to UV-induced damage, genome damage is associated with cell death in cells exposed to agents that mediate DNA damage through oxidative stress or alkylation as well (24–26).

Resistance of Snell dwarf fibroblasts to UV light–induced cell death might be caused by improved repair of DNA damage formed by irradiation. To test this idea, we used assays that measure recovery of transcription rates, and assays that measure formation and removal of DNA lesions themselves. We report here properties of Snell dwarf-derived fibroblasts that suggest an enhanced ability to repair UV-induced DNA lesions both in active genes and in the genome overall and that this enhanced repair correlates with a higher expression level of CSA and XPC involved in TCR and GGR, respectively.

Methods

Animal Subjects

Snell dwarf animals were *dw*/*dw* mice bred as the progeny of (DW/J × C3H/HeJ)-*dw*/+ females and (DW/J × C3H/HeJ)F1-*dw*/*dw* males. These sires had been previously treated with GH and thyroxine to increase body size and fertility. Littermates with the (+/*dw*) genotype were used as controls. Skin biopsies were taken from male mice 3–4 months of age.

Cell Culture

Fibroblast cultures were isolated as previously reported (11–13) in Dulbecco's modified Eagle medium (DMEM) supplemented with 20% heat-inactivated fetal bovine serum, antibiotics (penicillin at 100 U/mL and streptomycin at 100 μg/mL) and fungizone at 0.25 μg/mL (CM; complete medium). Initial cultures of cells derived from dwarf and littermate control (''Passage 0'') were grown to confluence (~95% confluence) with replacement of 2/3 of the CM on day 3 following seeding. On day 7 following seeding, cells were subcultured by trypsinization as previously reported (12,13) and seeded at a density of 1×10^4 cells/cm^2 flask surface area at each passage into tissue culture flasks of 75 cm^2 surface area to produce Passage 1 cultures. Further subculturing followed this protocol. For all assays, fibroblasts were used when they had reached the end of the second passage.

Assessment of Nascent Total RNA Synthesis Following UV Irradiation

Confluent, second passage cells were trypsinized and seeded into 96-well flat bottom tissue culture-treated microtiter plates in CM as described for UV resistance assays (11,12). After approximately 24 hours of incubation, cells were washed with 1X phosphate-buffered saline (PBS) and incubated in DMEM supplemented with 2% bovine serum albumin, antibiotics, and fungizone (SD medium; ''serum-deprived'') for approximately 24 hours. Following this period in SD medium, cells were washed, then irradiated with graded doses of UV-C light (254 nm) in 100 μL of warm Dulbecco's PBS (Gibco-Invitrogen, Carlsbad, CA). PBS was then aspirated, and 100 μL of fresh, warm SD medium was added to wells. To measure total RNA synthesis, 0.5 μCi of ^{3}H-uridine (MP Biomedicals, Solon, OH) was added to each well in 10 μL of SD medium at each time point presented. Following a 0.5-hour incubation with ^{3}H-uridine, cells were harvested onto glass-fiber filters using a 96-well FilterMate Harvester (Perkin-Elmer, Waltham, MA). Counts per minute (cpm) of incorporated ^{3}H-uridine was measured by liquid scintillation with MicroScint-O scintillation fluid (Perkin-Elmer) using a TopCount NXT scintillation counter (Perkin-Elmer). Additionally, identically treated cultures for all stresses were assayed for cell viability using WST-1 at the same time points following irradiation. All incubations were at 37°C in a humidified incubator with 5% CO_2 in air.

Assessment of Nascent Messenger RNA Synthesis Following UV Irradiation

Confluent, second passage cells were trypsinized, and 3×10^5 cells in 1 mL of CM were seeded into tissue culture-treated six-well plates (Corning Costar, Lowell, MA). After approximately 24 hours of incubation, cells were washed with 1X PBS and incubated in 1 mL of warm, fresh SD for approximately 24 hours. Following this period in SD medium, cells were washed and then irradiated with 10 J/m^2 UV light (254 nm) in 1 mL of warm Dulbecco's PBS. PBS was then aspirated, and 1 mL of fresh, warm SD medium was added to wells. To measure total RNA synthesis, 5 μCi of ^{3}H-uridine (MP Biomedicals) was added to each well in 100 μL of SD medium at each time point presented. Following a 0.5-hour incubation with ^{3}H-uridine, total RNA was isolated from each well (RNeasy Mini Kit; Qiagen, Valencia, CA). Total DNA was isolated from parallel cultures using the DNeasy kit (Qiagen); total DNA was quantified using an ND100 small volume spectrophotometer (Nanodrop, Wilmington, DE) and was used to normalize RNA samples to adjust for differences in cell survival. RNA from transcribed genes (messenger RNA, mRNA) was isolated by poly-A binding (Oligotex mRNA kit; Qiagen), then was bound to a glass-fiber filter, and the cpm of incorporated ^{3}H-uridine was measured as for total RNA above. All incubations were at 37°C in a humidified incubator with 5% CO_2 in air.

Measurement of UV Lesions in Genome by Enzyme-Linked Immunosorbent Assay

Confluent, second passage cells were trypsinized and seeded into dishes as for assessment of nascent mRNA

synthesis above. Following 24-hour incubation in SD, cells were irradiated as above and returned to SD medium. At the time points listed, and in cells that were not irradiated, genomic DNA was isolated using a DNeasy tissue kit (Qiagen) and stored in the supplied AE buffer. Genomic DNA was quantified using an ND100 spectrophotometer (Nanodrop) and diluted to a stock dilution of 40 μg/mL with 1X TE buffer (10 mM Tris–Cl pH 7.5, 1 mM EDTA). Enzyme-linked immunosorbent assay (ELISA) plates were prepared as per instructions from the vendor (MBL, Nakaku Nagoya, Japan) and as based on previous publications (27,28). In brief, 96-well polyvinyl chloride sample plates (Thermo Labsystems, Franklin, MA) were prepared by coating each well with 50 μL of 0.003% protamine sulfate (Sigma, St. Louis, MO) in distilled water; the plates were then dried at 37°C overnight. For measuring cyclobutane pyrimidine dimers (CPD) lesions, genomic DNA was diluted to 0.4 μg/mL in 1X PBS, and then denatured at 100°C for 10 minutes and chilled on ice for 15 minutes. Fifty microliters of the denatured, diluted genomic DNA was added to each of triplicate wells for DNA isolated from each cell line at each experimental time. For measuring 6-4 photoproducts (6-4PP) lesions, genomic DNA was diluted to 4 μg/mL and prepared similarly. Plates were then dried overnight at 37°C. For blocking, each well was washed five times with PBS-T (0.05% Tween-20 in 1X PBS) and then incubated with 2% fetal calf serum (FCS) in 1X PBS for 1 hour at 37°C. Wells were then washed five times with PBS-T and then incubated with 100 μL of primary antibodies for CPD or 6-4PP (29) at a dilution of 1:2000 in PBS for 1 hour at 37°C. Wells were then washed five times with PBS-T and incubated for 1 hour at 37°C with 150 uL of Biotin-F(ab′)$_2$ fragment of antimouse immunoglobulin G (IgG; Zymed, San Francisco, CA) diluted 1:2000 in 1X PBS. Wells were washed five times with PBS-T and then incubated for 1 hour at 37°C with 100 μL of peroxidase–streptavidin (Zymed) diluted 1:10,000 in PBS. Following this incubation, cells were washed five times with PBS-T and then washed once with citrate–phosphate buffer (pH 5.0). To provide quantitation, 100 μL of substrate solution (o-phenylenediamine [Zymed], H_2O_2, citrate–phosphate buffer, pH 5.0) was added to each well and incubated 30 minutes at 37°C. To stop the reaction, 50 μL of 2M H_2SO_4 was added, and plates were read by determining the absorbance at 492 nM on a SpectraMax Plus spectrophotometer (Molecular Devices, Sunnyvale, CA).

Quantitative Polymerase Chain Reaction

Confluent, second passage cells were trypsinized and seeded into dishes as for assessment of nascent mRNA synthesis above. Following 24 hours incubation in SD, cells were irradiated as above and returned to SD medium. At the time points listed, and in cells that were not irradiated, genomic DNA was isolated using a DNeasy tissue kit (Qiagen) and stored in the supplied AE buffer. Genomic DNA was quantified using PicoGreen double-stranded DNA dye (Invitrogen, Carlsbad, CA) according to the manufacturer's instructions and diluted to a final concentration of 3 ng/μL in 1X TE buffer. Quantitative polymerase chain reactions (PCRs) were run as previously described with primers for the 6.5-kb fragment from the 5′ flanking region up to exon I of mouse DNA polymerase beta (*Pol*β) or for the 8.7 kb fragment from the 5′ flanking region of mouse beta-globin (β*glo*) (30–32). PCRs were run using the GenAmpXL PCR kit (Applied Biosystems, Foster City, CA) for 30 cycles in an MJ Research PTC-100 Thermocycler (MJ Research, Waltham, MA). PCR samples were quantified using PicoGreen dye according to the manufacturer's instructions.

Western Blot Analysis of NER Proteins

Confluent, second passage cells were trypsinized and seeded into dishes as for assessment of nascent mRNA synthesis above. Total cellular protein was isolated from cells incubated in CM for 24 hours following trypsinization and from cells that had undergone an additional 24-hour incubation in SD medium. Cells were lysed in a modified RIPA buffer and stored at −20°C until analysis. Total protein content was measured by the Pierce bicinchoninic acid (BCA) assay (BioRad, Hercules, CA). For blots, 20 μg of total cellular protein extract was prepared in 6X sodium dodecyl sulfate (SDS) sample buffer, subjected to SDS-polyacrylamide gel electrophoresis, and transferred to polyvinylidene difluoride (PVDF) membrane (Millipore, Billerica, MA). The membrane was blocked in 3% BSA, 0.1% Tween 20 in 1X PBS. CSA, XPC, XPF, and XPG antibodies (Santa Cruz Biotechnology, Santa Cruz, CA) were used at a dilution of 1:1000 in 3% BSA, 0.1% Tween 20 in 1X PBS. Actin primary antibody (Sigma) was used at a dilution of 1:5000 in 3% BSA, 0.1% Tween 20 in 1X PBS. Alkaline phosphatase–conjugated secondary antibodies (Santa Cruz Biotechnology) were then used at a dilution of 1:10,000 in 1% BSA, 0.1% Tween 20 in 1X PBS, and bands were detected using enhanced chemifluorescence (ECF) reagent (GE Healthcare, Piscataway, NJ) and fluorescence scanning (Storm System; Molecular Dynamics, Piscataway, NJ). Band intensities were measured using the ImageQuant software package (Molecular Dynamics).

Data Analysis and Statistics

For transcription assays, differences between dwarf- and control-derived cell lines in their uridine incorporation were analyzed separately at each time point by paired *t* test. For recovery of transcription, differences between dwarf- and control-derived cell lines in the time to recovery were analyzed by Wilcoxon's nonparametric *t* test. For ELISA assays, differences between dwarf and control DNA in the intensity of substrate signal were analyzed at each time point by paired *t* test. For quantitative PCR (QPCR), differences in the quantity of DNA in each amplification reaction between samples using dwarf and control DNA were analyzed at each time point by paired *t* test. For Western blots, the intensity of each band was normalized to the corresponding β-actin, and differences in these values between dwarf and control were measured under each condition by paired *t* test. For all, differences were reported as statistically significant if $p < .05$.

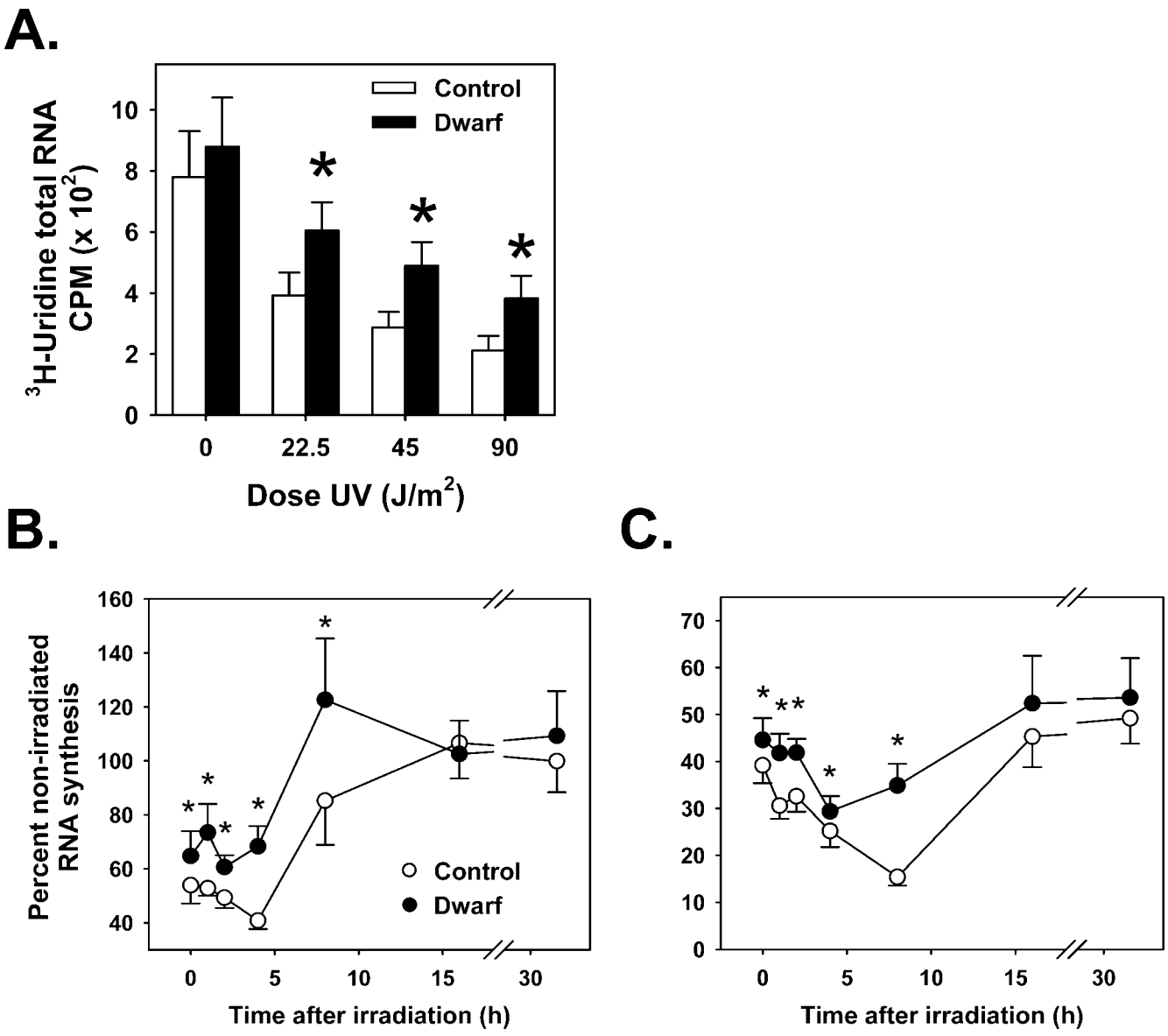

Figure 1. Fibroblasts from Snell dwarf mice show less inhibition of total RNA synthesis following ultraviolet (UV) irradiation than do fibroblasts from control mice. **A,** Cell lines isolated from nine individual Snell dwarf mice (*filled bars*) and nine individual controls (*open bars*) were assayed for ^{3}H-uridine incorporation into total RNA as a function of dose of UV irradiation. Cells were irradiated then incubated with ^{3}H-uridine for 0.5 hours prior to total RNA collection. Error bars represent standard error of the mean (*SEM*). *$p < .05$ for paired *t* test between genotypes for each individual dose of UV light. CPM, counts per minute. **B,** Each circle represents the average ^{3}H-uridine incorporation of UV-irradiated (22.5 J/m^2) cell lines from nine Snell dwarf mice (*filled circles*) and from nine controls (*open circles*) relative to their respective nonirradiated controls. Cells were irradiated and then incubated in serum-deprived (SD) medium for times indicated on *x*-axis prior to total RNA collection. Error bars represent *SEM*. *$p < .05$ for paired *t* test between genotypes for each individual dose of UV light. **C,** As in (**B**) for 45 J/m^2 dose of UV light.

Results

Fibroblasts from Snell dwarf mice are particularly resistant to the lethal effects of UV light and of MMS (16,17), agents that cause cell death primarily through the induction of DNA lesions. Because cell death induced by these agents is also associated with the inhibition of RNA synthesis, we measured transcription rates and their relative recovery in dwarf- and control-derived fibroblasts. Total RNA synthesis rates were equivalent in dwarf- and control-derived cells that had not been irradiated (Figure 1A). However, in cells that had been irradiated and then immediately incubated for 0.5 hours with ^{3}H-uridine, dwarf-derived cells exhibited significantly less reduction of ^{3}H-uridine incorporation for each of three doses of UV light tested, suggesting that RNA synthesis was less inhibited in fibroblasts from dwarf animals in the immediate aftermath of irradiation compared to control cells (Figure 1A). It is unlikely that these results are due to differences in cell death because cell viability was similar for both genotypes at these time points as measured by WST-1 assay

Table 1. ^{3}H-Uridine Incorporation Following UV Irradiation Is Greater in Dwarf-Derived Fibroblasts

	Average Percent Control CPM of ^{3}H-Uridine Uptake, Normalized by Experiment Day (*SEM*)					
	22.5 J/m^2 UV light			45 J/m^2 UV light		
Time Following UV, h	Control	Dwarf	Paired *t* test *p*	Control	Dwarf	Paired *t* test *p*
No UV	100 (9)	112 (14)	.24	100 (9)	112 (14)	.24
0	100 (11)	171 (23)	.005*	100 (12)	174 (15)	.001*
0.5	100 (9)	140 (14)	.02*	100 (9)	135 (12)	.03*
1	100 (10)	120 (8)	.05*	100 (10)	142 (20)	.04*
2	100 (8)	157 (24)	.02*	100 (11)	152 (16)	.01*
4	100 (10)	226 (14)	<.001*	100 (14)	142 (18)	.04*
8	100 (8)	151 (14)	.01*	100 (10)	217 (29)	.002*
16	100 (6)	112 (8)	.16	100 (8)	133 (23)	.08
32	100 (5)	131 (17)	.08	100 (8)	90 (20)	.34

Notes: For each time point, cells lines from nine individual animals of each genotype were assayed for ^{3}H-uridine incorporation following ultraviolet (UV) irradiation. An average value for control cells at each time point was calculated, and both dwarf and control values were normalized to this.

*$p < .05$.

CPM = counts per minute; *SEM* = standard error of the mean.

(data not shown). Such a finding might reflect either differences in immediate DNA repair or in the ability of RNA polymerase to bypass lesions (33).

To test if there was a difference in the recovery of RNA synthesis over time, ^{3}H-uridine incorporation was measured at varying time points after UV irradiation. Figure 1B shows results for cells exposed to 22 J/m^2, and Figure 1C shows results for cells exposed to 45 J/m^2. These assays use the rate at which RNA synthesis recovers from inhibition as an estimation of the rate of DNA repair (19). At either of the two UV doses used, cell lines from dwarf mice showed a higher rate of RNA synthesis at most times following irradiation compared to control cells (Figure 1B and C; Table 1). Furthermore, we recorded, for each cell line, the time point at which recovery of RNA synthesis began after UV exposure and found that the time needed for recovery of RNA synthesis was significantly lower in dwarf-derived cell lines for each of two doses of UV light (Table 2). It should be noted that following a 22.5 J/m^2 dose of UV light, both dwarf and control cells recover RNA synthesis to levels similar to those of nonirradiated cells, whereas recovery following 45 J/m^2 UV light is not complete for either dwarf or control cells (Figure 1B and C). Higher doses of UV light led to irreversible inhibition of RNA synthesis (data not shown) and subsequent cell death. These results show that cells from dwarf mice recover RNA synthesis faster than control cells following UV irradiation, and suggest that repair of UV lesions may occur more rapidly in cells from dwarf animals than in control cells, at least in regions of the genome from which RNA is transcribed.

In a second series of studies, we used ELISA methods to measure two of the lesions formed in DNA by UV-C light, CPD and 6-4PP (34). We found no difference in the background levels of CPD and 6-4PP within the genomic DNA isolated from dwarf- and control-derived cells (Figure 2A and B). As expected, UV light (22.5 J/m^2) induced the formation of both CPD and 6-4PP in genomic DNA isolated immediately after irradiation, and there was no difference between dwarf and control cells in CPD or 6-4PP (Figure 2A and B). These data suggest that genomic DNA of both cell lines is equally susceptible to the energy of UV light and that the difference in transcription and cell survival cannot be explained by differences in physical protection from UV light. We next evaluated the time course of removal of these lesions from genomic DNA and found that there was no difference in the rate of lesion removal between dwarf and control cell lines at early time points. However, dwarf-derived cells did show a significantly lower level of CPD lesions in DNA isolated from cells 24 hours after UV irradiation, and there was a trend of this also at 8 hours (Figure 2C). Similar to CPD lesions, the dwarf cells showed a significantly better removal of 6-4PP by 24 hours after UV irradiation compared to control cells (Figure 2D).

The cytotoxicity of UV light is closely correlated with the preferential removal of UV-induced lesions from actively transcribed, protein-encoding genes; thus the synthesis of mRNA can be used as an indirect measure of TCR of these regions (19). Incorporation of ^{3}H-uridine into mRNA was measured after UV irradiation to provide an estimate of TCR. In contrast to the results for total RNA synthesis, we

Table 2. Inhibition of Transcription Is Repaired More Rapidly in Snell Dwarf-Derived Fibroblasts

UV Dose	Genotype	Sample Size	Average Time to Recovery, h	*SEM*	Wilcoxon *p*
22.5 J/m^2	Snell dwarf	9	5.3	0.8	
	Control	9	8.9	1.2	.017
45 J/m^2	Snell dwarf	9	10.7	1.4	
	Control	9	19.6	2.4	.011

Notes: Average time to recovery represents the average time at which the difference in RNA synthesis between ultraviolet (UV)-irradiated and nonirradiated cells begins to diminish, as an index of the speed of removal of transcription-blocking UV lesions. Wilcoxon *p* represents the *p* value calculated for a Wilcoxon nonparametric test.

SEM = standard error of the mean.

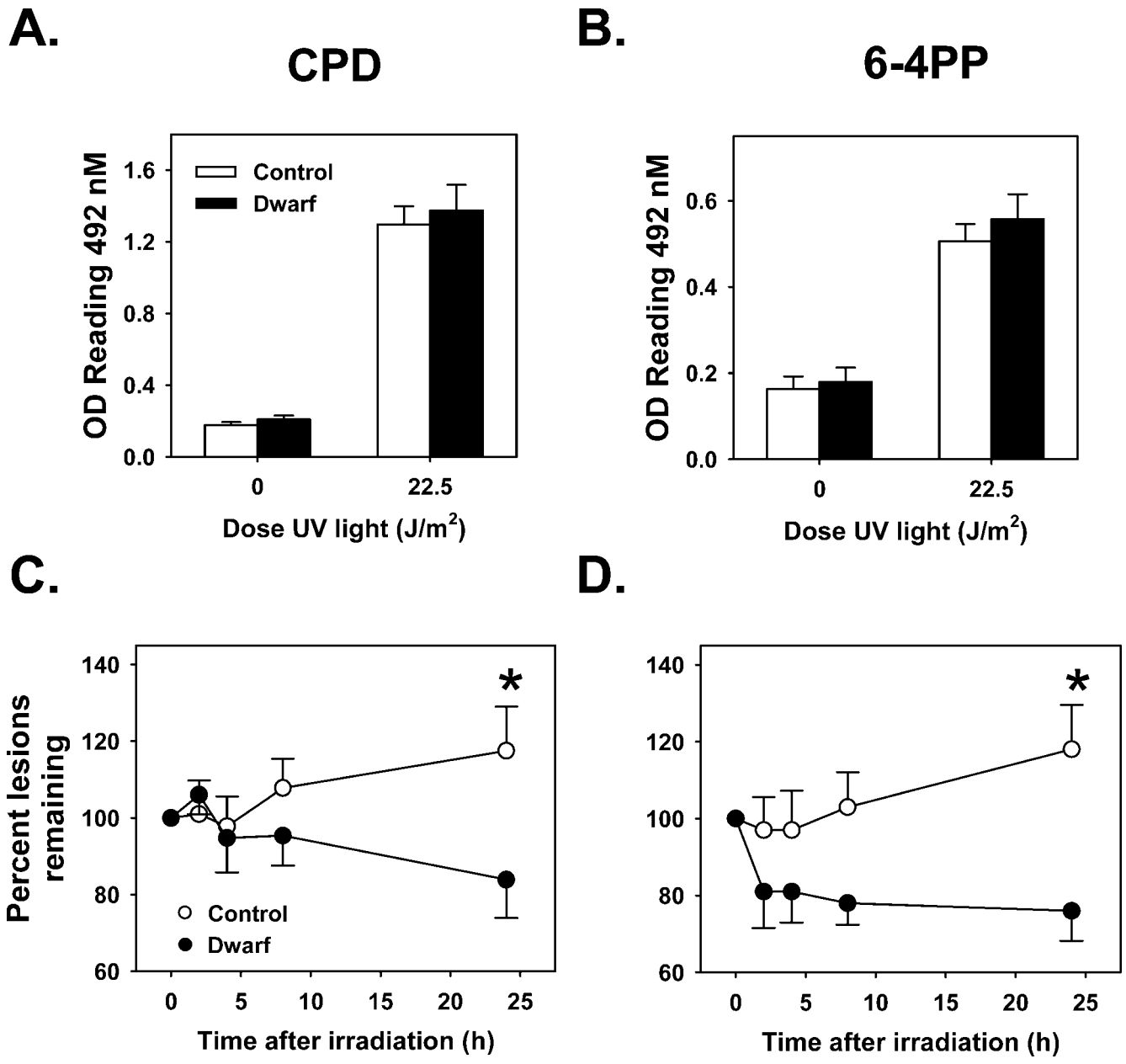

Figure 2. Fibroblasts from Snell dwarf mice remove significantly more cyclobutane pyrimidine dimers (CPDs) and 6-4 photoproducts (6-4PPs) from the whole genome over time compared to control cells. **A,** Average value quantified by spectrophotometer of the presence of CPD lesions in genomic DNA from cell lines isolated from 11 individual Snell dwarf mice (*filled bars*) and 11 individual controls (*open bars*). Genomic DNA was isolated from nonirradiated cells or immediately following irradiation as indicated by *x*-axis. Error bars represent standard error of the mean (*SEM*). UV, ultraviolet; OD, optical density. **B,** Presence of 6-4PP presented as in (**A**). **C,** Average CPD enzyme-linked immunosorbent assay result for genomic DNA isolated from cells at the indicated times following irradiation, relative to the results presented in (**A**). *Filled circles:* results from cell lines derived from 11 different Snell dwarf mice; *open circles:* results from 11 controls. Error bars represent *SEM*. *$p < .05$ for paired *t* test between genotypes at that time point. **D,** Presence of 6-4PP presented as in (**C**).

found no significant difference between dwarf- and control-derived cell lines in the inhibition of mRNA synthesis measured immediately after irradiation with a dose of 10 J/m^2 and a 0.5-hour incubation with ^{3}H-uridine (Figure 3A). Nor was there any significant difference between dwarf and control in their relative mRNA synthesis when measured 2 or 4 hours following UV treatment (Figure 3B). However, the level of ^{3}H-uridine incorporation into mRNA in dwarf-derived cells rose rapidly between 4 and 8 hours and reached nearly double that found in control-derived cells at 8 hours after UV irradiation (Figure 3B). The synthesis of mRNA was also higher in dwarf-derived cells at 24 hours after irradiation, although these results did not reach statistical significance ($p < .06$). Together, these results show that recovery of UV-induced inhibition of mRNA synthesis occurs relatively earlier in dwarf-derived cell lines, suggesting that cells from dwarf mice have a more efficient TCR compared to control cells.

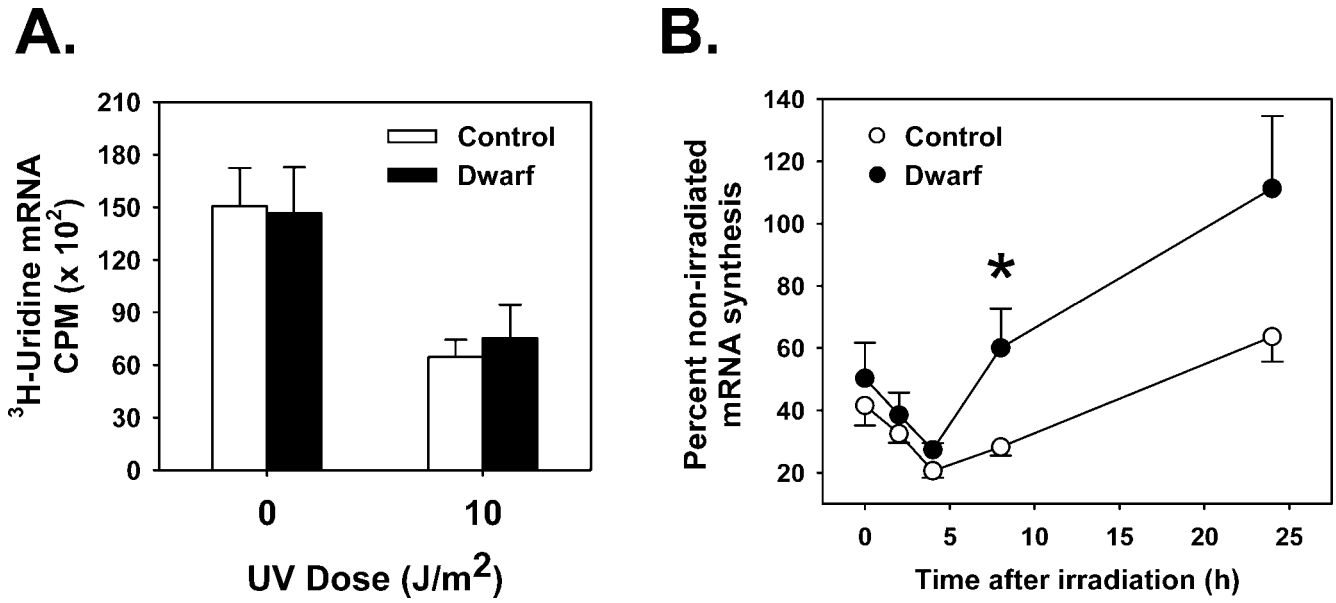

Figure 3. Faster recovery of messenger RNA (mRNA) synthesis following ultraviolet (UV) irradiation in fibroblasts from Snell dwarf compared to control cells. **A,** Cell lines isolated from six individual Snell dwarf mice (*filled bars*) and six individual controls (*open bars*) were assayed for ^{3}H-uridine incorporation into mRNA following UV irradiation. Cells were irradiated (or not) then incubated with ^{3}H-uridine for 0.5 hours prior to mRNA collection. Error bars represent standard error of the mean (*SEM*). CPM, counts per minute. **B,** Each circle represents the average ^{3}H-uridine incorporation of UV-irradiated cell lines from six Snell dwarf mice (*filled circles*) and from six controls (*open circles*) relative to their respective nonirradiated controls. Cells were irradiated and then incubated in serum-deprived (SD) medium for time indicated on *x*-axis prior to total RNA collection. Error bars represent *SEM*. *$p < .05$ for paired *t* test between genotypes for each individual UV dose.

To directly test whether UV lesions in actively transcribed genes are removed faster in dwarf cells than in control cells, we used QPCR to assess the levels of lesions at different times after UV irradiation in two specific genes, *Pol*β and β*glo*. The assay measures the extent to which DNA lesions prevent the progress of DNA polymerase in a PCR amplification of the specific DNA sequences of interest; amplification of DNA containing unrepaired lesions is expected to be less than that of nonirradiated or repaired DNA (30–32). In unirradiated cells, we found no difference between dwarf and control in the amount of amplification of a region of *Pol*β (Figure 4A), which is actively transcribed in fibroblasts, or in the amount of amplification of a region of β*glo* (Figure 4B), a gene that is not transcribed in fibroblasts (a negative control). Compared to nonirradiated cells, *Pol*β and β*glo* amplification were inhibited approximately 50% in both dwarf and control cells when using genomic DNA isolated immediately after 10 J/m^2 UV light (Figure 4, A and B). Amplification of *Pol*β increased with time after irradiation, indicating that UV lesions were being removed from these sequences (Figure 4C). Amplification of *Pol*β tended to be higher in dwarf-derived cells over time, although the results did not reach statistical significance. For β*glo*, we found no evidence for any change in relative amplification over time and no difference between dwarf and control, suggesting that lesions were not being removed from this nontranscribed gene fragment (Figure 4D). Because there was no measurable repair in the β*glo* gene, it might also be possible that the region of the gene amplified by this assay is completely refractory to repair for reasons unrelated to the Snell dwarf phenotype.

Seeking molecular explanations for the differences between dwarf and control cells in the repair of UV-induced damage, we used immunoblotting to measure the protein levels of some of the enzymes important in NER. XPC is the DNA binding subunit of the XPC-hHR23B complex (35) and has affinity for multiple sites of genomic damage, in particular bulky adducts like 6-4PP that introduce helical distortions in the nucleic acids (36–39). Recognition of lesions repaired by TCR occurs by recruitment of the CSA and CSB proteins to the site of the stalled RNA polymerase II (RNAPII) complex (19,40,41). XPF and XPG are endonucleases that incise on the 3′ and 5′ side of the damaged DNA region, respectively (42,43). Lysates were prepared in two conditions: (i) from cells grown to confluence in complete medium and (ii) from confluent cells that had been further incubated for 24 hours in medium without serum. This serum-free condition was evaluated because the difference in stress resistance between dwarf and normal cells is most pronounced under these circumstances (11), and because lysates from serum-deprived cells had been used for the DNA repair assays presented above. We saw no difference in the expression of any of four NER proteins using lysates from cells grown to confluence in medium containing serum (Figure 5). In cells that had been incubated in serum-deprived medium, however, we found significantly more XPC and CSA expression in dwarf-derived cell lines compared to control cells. There was no difference between serum-deprived dwarf and control cells in their expression of XPG or XPF.

Discussion

The energy of UV light is absorbed by DNA and causes the formation of bulky genomic lesions in DNA. These lesions play a significant role in cytotoxicity, mutagenesis,

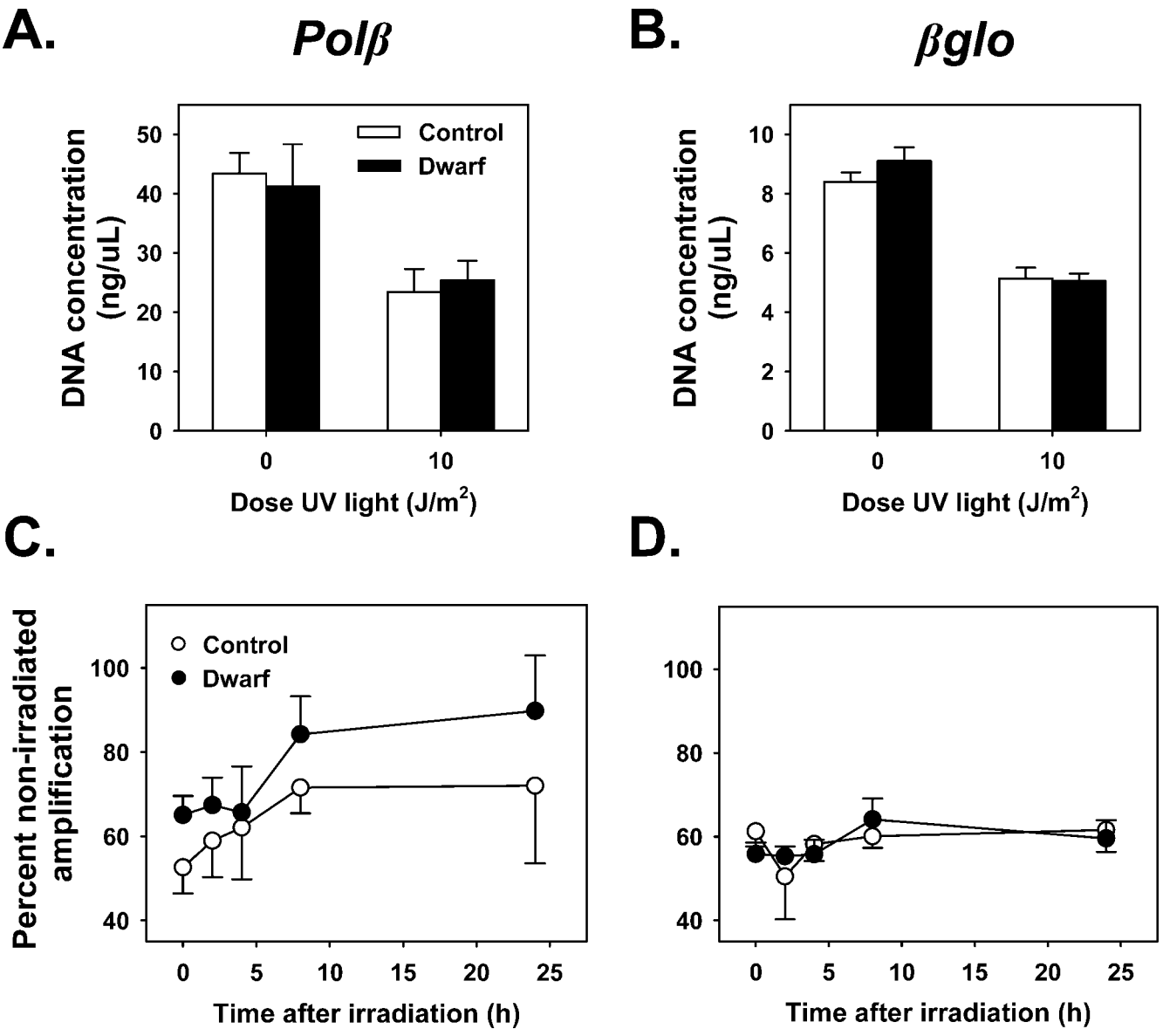

Figure 4. There is no significant difference in the formation or removal of ultraviolet (UV) lesions from two specific genes as measured by amplification of quantitative polymerase chain reaction (QPCR) products using genomic DNA isolated from irradiated cells. **A,** Average concentration of DNA measured following QPCR of *Pol*β using genomic DNA from nonirradiated cells and genomic DNA isolated immediately following UV irradiation (*x*-axis). Bars represent the average results from the genomic DNA of cell lines isolated from six individual Snell dwarf mice (*filled bars*) and six individual control mice (*open bars*). Error bars represent standard error of the mean (*SEM*). **B,** As in (**A**) for QPCR of β*glo*. **C,** Each circle represents the average concentration of QPCR products for *Pol*β using genomic DNA from cells irradiated and then incubated in serum-deprived (SD) medium for time indicated on *x*-axis prior to isolation of DNA. *Filled circles:* results of genomic DNA from cell lines isolated from six Snell dwarf mice; *open circles:* results from six control mice. Error bars represent *SEM*. **D,** As in (**C**), for QPCR of β*glo*.

and the development of neoplasia in mammals (44,45). Therefore, the rapid and efficient repair of these lesions is of critical importance to cell survival and tumor suppression (15). Further, differences in the resistance to UV-induced cell death might result from differential response and repair of UV-induced DNA lesions (23,46). We have previously found that skin-derived fibroblasts from the long-lived Snell dwarf mice, and related long-lived mouse models, are resistant to the cytotoxic effects of UV light (11,12). Here we report that the enhanced survival of dwarf-derived fibroblasts is accompanied by an enhanced ability to repair UV lesions both within active genes and within the genome as a whole and an enhanced recovery of mRNA synthesis following UV irradiation. Further, we find that differences in DNA repair are associated with expression levels of NER proteins thought to play roles in the cellular recognition of blocked RNAPII complexes as well as global genomic DNA lesions.

Cell death caused by UV light is, at least in part, due to the cytotoxicity of bulky UV-induced lesions formed within actively transcribing genes; these adducts block the progression of RNA polymerase and inhibit transcription

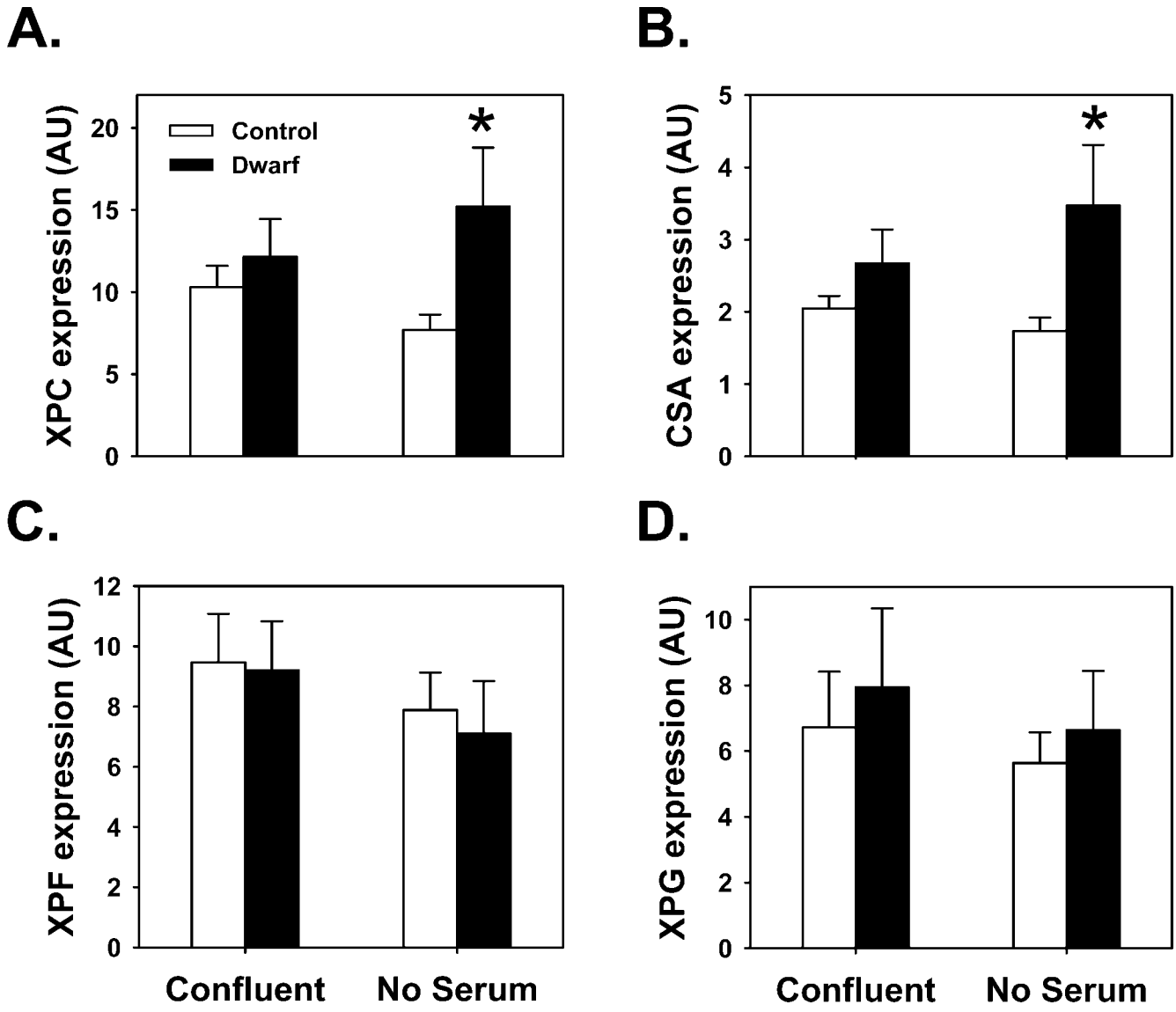

Figure 5. Fibroblasts from Snell dwarf mice express higher levels than do control cells of XPC and CSA following serum deprivation. For each graph, the *x*-axis represents the cell growth condition from which total cell protein lysates were made. *Bars* represent the average expression of the indicated protein as measured by immunoblot of 20 μg of protein from total cell lysates and normalized to β-actin expression. *Filled bars:* average expression of the indicated protein in cell lines isolated from seven individual Snell dwarf mice; *open bars:* average expression in cell lines isolated from seven control mice. Error bars represent standard error of the mean. $*p < .05$ for paired *t* test between genotypes for that particular treatment. **A,** Cumulative results from immunoblots for XPC. **B,** Cumulative results from immunoblots for CSA. **C,** Cumulative results from immunoblots for XPF. **D,** Cumulative results from immunoblots for XPG. AU = Arbitrary Units.

(18,23). Cells from donors with TCR defects, such as those from patients with Cockayne's syndrome (CS) or xeroderma pigmentosa complementation group A (XP-A), have poor recovery of mRNA synthesis following UV and undergo apoptosis at relatively low doses of UV irradiation (23,47). In addition, cells deficient in pRb, a protein thought to play a role in GGR, also show UV sensitivity and poor recovery of mRNA synthesis following UV irradiation (46,48). These data suggest that UV lesion repair regulates the cell's sensitivity to irradiation and hint at a potential mechanism for the resistance of Snell dwarf cells to DNA-damaging agents. The relatively rapid recovery of mRNA synthesis after UV irradiation (Figure 3B), an index of TCR, provides a plausible explanation for the resistance of Snell dwarf cells to death induced by UV. Our QPCR data on repair of UV-induced lesions in *Pol*β, an actively transcribed gene, are consistent with this idea, although the differences between normal and dwarf mice were not statistically significant in this assay. Because this assay measures removal of lesions from both strands of the sequence to be amplified, removal specifically from the transcribed strand will be somewhat obscured; therefore, this assay will underestimate TCR.

We found relatively little removal of UV-induced CPD and 6-4PP, though there were significantly fewer CPDs and 6-4PPs in DNA from dwarf cells 24 hours after irradiation. This relatively modest level of repair is consistent with that

reported for other groups using rodent-derived cell lines (49–51) and likely reflects the well-documented deficiency of GGR in rodents (52). The low level of GGR is consistent with our QPCR data on a β*glo,* a gene that is not transcribed in fibroblasts: We see no recovery in amplification of β*glo* DNA in the 24 hours following irradiation, suggesting that no UV lesions have been repaired. However, a region of a transcribed gene, *Pol*β, was repaired much more effectively with amplification recovering slowly in the 24 hours after irradiation. Amplification of *Pol*β sequences returned to 90% (±13% standard error of the mean [*SEM*]) of nonirradiated levels in dwarf cells, compared to 72% (±18% *SEM*) in control cells at 24 hours, suggesting that more lesions had been repaired in dwarf-derived cells, although the difference is not statistically significant.

We found no evidence for a difference between dwarf and control cells in the formation of UV damage immediately after irradiation within either the whole genome as measured by ELISA or of specific regions as measured by QPCR. There was also no difference in the synthesis of mRNA measured at the earliest time point, 0.5 hours following irradiation. These observations are all consistent with the working hypothesis that DNA in dwarf and control cells is equally vulnerable to the immediate effects of UV exposure. In contrast, we did note that transcription of total RNA was significantly higher in dwarf-derived cells when measured in the 30 minutes immediately after UV exposure. This disparity raises the possibility that polymerases for non-mRNA transcripts may be able to bypass UV lesions to differing degrees in dwarf and control cells. There are few data on RNAPI or RNAPIII, but in Chinese hamster ovary cells and in human cells, recovery of RNA synthesis has been shown to precede the strand-specific removal of photolesions from the genome, presumably because RNAPII is able to bypass the remaining lesions (33,53). Alternatively, it seems possible that some portion of the DNA damage is repaired so rapidly after irradiation that differences between dwarf and control cells can be observed even within the 30-minute incubation needed to measure the rate of ^{3}H-uridine incorporation.

Our data suggest that the onset of repair following irradiation occurs more rapidly in cells from Snell dwarf mice than in cells from control mice. The cellular recognition of lesions within the genome has been proposed as the rate-limiting step of NER (54) in part because of the large number of bases in the genome that must be scanned for many types of damage and also because of the physical limitations of the sequential recruitment of repair proteins to the site of damage (55). Cells expressing more of the NER proteins required for recognition of UV lesions may thus be able to repair lesions more rapidly than those expressing proteins at lower levels. We found that dwarf-derived cells expressed higher levels of the proteins XPC and CSA than did control cells, when evaluated after 24-hour incubation in serum-free medium. It is unclear why serum deprivation might affect the expression of these proteins differently in Snell dwarf-derived cells. It may be that the removal of serum from the growth medium represents a stressful condition that upregulates the expression of proteins involved in repair of damaged macromolecules.

The binding of XPC to UV lesions is thought to guide the formation of the NER complex for the execution of GGR (56–58). CSA and CSB bind in concert to the stalled RNAPII and facilitate the assembly of the TCR complex, thereby acting as the de facto recognition proteins for TCR (59–62). It has also been proposed that CSA protects the stalled RNAPII and CSB from proteasomal degradation (40,63). Higher levels of CSA may thus stabilize the intact TCR complex, leading to more efficient TCR. Interestingly, there was no difference between dwarf and control in the expression of the NER excision proteins XPF and XPG (42,43), suggesting that differences in DNA repair might be mediated by differences in the level of proteins involved in the rate-limiting steps of repair and not necessarily upregulation of the entire pathway. It would be of interest to explore if overexpression of these proteins in cell lines, or in transgenic mouse models, alters cellular stress resistance and organismic longevity.

Dwarf-derived cells were found to repair UV lesions more rapidly in both the whole genome and, to some extent, in transcribed regions. Unrepaired UV lesions located within transcribed genes can cause cell death (17–20, 23) and are thus plausible explanations for differential resistance to UV-induced cell death. Lesions in the 95% of the genome that is not transcribed in a given cell type are considered primarily mutagenic and are of little consequence to survival of the cell in the short term (19). The difference in global repair of CPD and 6-4PP presented in Figure 2 may contribute to the comparatively low incidence and the delay of neoplasia in dwarf mice (5,64). The contributions of NER deficits to deficiency in DNA repair is well documented, but less is known about the control of DNA fidelity over the long term and the balance between cell death and transformation that modulates incidence and progression of neoplastic lesions. There are some limited data suggesting that Snell dwarf mice are resistant to DNA damage, in vivo; treatment with x-ray or mitomycin C results in fewer mutagenic lesions in erythrocytes, bone marrow cells, and spermatogonia of Snell dwarf mice (65,66). Data on the formation and repair of CPD and 6-4PP in the DNA of skin cells of irradiated dwarf and control mice would provide a useful in vivo correlate for our in vitro observations. There is also some suggestion that the development of neoplasia induced by mutagens and implanted tumors is diminished in Snell dwarf mice (67–70). Therefore, it would be of interest to test if Snell dwarf mice were resistant to the development of cancer induced by an assortment of agents that induce repairable DNA damage, including UV light.

We have previously shown that cells from Snell dwarf mice are resistant to cell death caused by another DNA-damaging agent, the DNA alkylator MMS (12). Similarly, studies of MMS resistance in cells from Ames dwarf and GH receptor knockout mice showed greater resistance in mutants than in controls, but the effect did not reach statistical significance in tests with 4–6 pairs of cell lines (Salmon A, Miller R, unpublished data, 2005). Although NER may play some part in the repair of MMS lesions, it is generally thought that the methylated bases caused by MMS are repaired by the process of base excision repair (54,71). Thus, it may be that multiple forms of DNA repair processes

are upregulated in cells of long-lived mutant mice. Therefore, it would be of interest to test whether cell lines from long-lived mice show increased rates of repair of alkylated DNA through base excision repair.

Many have speculated that the loss of genome integrity may contribute to aging, and that differences in DNA repair processes might modulate the rate of aging (72,73). Age-related decline has been observed in the ability of many species to repair UV damage as measured by unscheduled DNA synthesis, including human and mouse (74–77). More interestingly, a number of studies have suggested that the repair of UV lesions is correlated with longevity across mammals (78–80). However, our own data and that of others suggest that there is much variation among rodent species of different longevities in their response to UV damage (81,82). Caloric restriction, which extends life span in most tested species (83), has also been shown to improve repair of DNA after UV irradiation. For example, dietary restriction enhances UV repair of kidney cells in rats (84), hepatocytes in rats and mice (76,84), fibroblasts derived from the lung and the skin of rats (85,86), and splenocytes in mouse (87). Although these studies measured GGR, it has been shown that the removal of CPD lesions from specific genes is enhanced in the hepatocytes of calorie-restricted rats, suggesting enhanced TCR (88).

It is not clear how a better system of UV lesion repair may directly contribute to the extended life span of diet-restricted animals or of the Snell dwarf mouse reported here. The large number of cell types showing greater repair capacity in calorie-restricted models suggests global protection from damage. It may be that enhanced DNA repair contributes to the decreased accumulation of DNA damage in long-lived animals, which could lead to diminished cell senescence (89), diminished cell loss by apoptosis (90), diminished p53 induction (91), or diminished development of neoplastic cells (15). In contrast, some evidence has been presented that suggests that high levels of global damage do not adversely affect longevity or age-related physiological decline. For instance, mice lacking the mismatch repair gene *Pms2* have high mutation frequencies, but no change in life span and only a slight increase in carcinogenesis (92). Similarly, mice lacking the antioxidant manganese superoxide dismutase show high levels of oxidative lesions to both nuclear and mitochondrial DNA, have higher incidences of multiple tumor types, but have the same life span as their controls (93). Lastly, the maximum life span of naked mole-rats is approximately 8 times longer than that of mice, and no incidence of spontaneous cancer has ever been reported, yet their tissues show significantly more DNA oxidation than those in mice (94). It may well be that the connections between DNA repair and longevity are somewhat indirect and limited to some shared mechanisms of the repair of particular types or locations of DNA damage.

This study suggests mechanisms that may help explain the longevity and low cancer incidence in hypopituitary dwarf mice. By expressing a higher level of CSA protein involved in TCR, dwarf cells remove cytotoxic transcription-blocking lesions faster than do cells from control mice, leading to a faster recovery of mRNA synthesis after insult. Under some circumstances, faster repair might protect cells from apoptosis, and thus preserve function of tissues in which cell replacement is limiting. Dwarf cells also express high levels of XPC, which enhances the removal of mutagenic lesions by GGR; removal of these lesions might contribute to the low cancer incidence in dwarf mice (5,95). By enhancing both TCR and GGR without losing the balance between these repair pathways, dwarf mice enjoy longevity without paying the price of increased cancer incidence. Much remains to be learned, however, about the ways in which the endocrine abnormalities of the Snell dwarf mouse lead to long-lasting improvements in DNA repair pathways, about how these pathways are coupled with improved resistance to other forms of lethal and metabolic stress (11–13), and about the extent to which similar stress resistance might alter the properties of other cell types within the dwarf mouse.

Acknowledgments

This work was supported by National Institute on Aging grants AG023122 and AG054624, as well as by grant T32-AG000114 (to ABS).

We thank Dr. Bennett Van Houten for assistance with quantitative PCR assays and Maggie Lauderdale and Jessica Sewald for assistance with animal husbandry.

Correspondence

Address correspondence to Richard A. Miller, MD, PhD, Room 3001, BSRB Box 2200, 109 Zina Pitcher Place, Ann Arbor, MI 48109-0940. E-mail: millerr@umich.edu

References

1. Camper SA, Saunders TL, Katz RW, Reeves RH. The Pit-1 transcription factor gene is a candidate for the murine Snell dwarf mutation. *Genomics*. 1990;8:586–590.
2. Bartke A, Coschigano K, Kopchick J, et al. Genes that prolong life: relationships of growth hormone and growth to aging and life span. *J Gerontol Biol Sci*. 2001;56A:B340–B349.
3. Flurkey K, Papaconstantinou J, Miller RA, Harrison DE. Lifespan extension and delayed immune and collagen aging in mutant mice with defects in growth hormone production. *Proc Natl Acad Sci U S A*. 2001;98:6736–6741.
4. Silberberg R. Articular aging and osteoarthritis in dwarf mice. *Pathol Microbiol (Basel)*. 1972;38:417–430.
5. Vergara M, Smith-Wheelock M, Harper JM, Sigler R, Miller RA. Hormone-treated Snell dwarf mice regain fertility but remain long-lived and disease resistant. *J Gerontol Biol Sci Med Sci* 2004;59A: 1244–1250.
6. Ikeno Y, Bronson RT, Hubbard GB, Lee S, Bartke A. Delayed occurrence of fatal neoplastic diseases in Ames dwarf mice: correlation to extended longevity. *J Gerontol Biol Sci Med Sci*. 2003;58A: 291–296.
7. Johnson TE, Henderson S, Murakami S, et al. Longevity genes in the nematode *Caenorhabditis elegans* also mediate increased resistance to stress and prevent disease. *J Inherit Metab Dis*. 2002;25:197–206.
8. Lin YJ, Seroude L, Benzer S. Extended life-span and stress resistance in the *Drosophila* mutant methuselah. *Science*. 1998;282:943–946.
9. Migliaccio E, Giorgi M, Mele S, et al. The p66shc adaptor protein controls oxidative stress response and life span in mammals. *Nature*. 1999;402:309–313.
10. Holzenberger M, Dupont J, Ducos B, et al. IGF-1 receptor regulates lifespan and resistance to oxidative stress in mice. *Nature*. 2003; 421:182–187.
11. Murakami S, Salmon A, Miller RA. Multiplex stress resistance in cells from long-lived dwarf mice. *FASEB J*. 2003;17:1565–1566.

12. Salmon AB, Murakami S, Bartke A, Kopchick J, Yasumura K, Miller RA. Fibroblast cell lines from young adult mice of long-lived mutant strains are resistant to multiple forms of stress. *Am J Physiol Endocrinol Metab*. 2005;289:E23–E29.
13. Leiser SF, Salmon AB, Miller RA. Correlated resistance to glucose deprivation and cytotoxic agents in fibroblast cell lines from long-lived pituitary dwarf mice. *Mech Ageing Dev*. 2006;127:821–829.
14. Maynard SP, Miller RA. Fibroblasts from long-lived Snell dwarf mice are resistant to oxygen-induced in vitro growth arrest. *Aging Cell*. 2006;5:89–96.
15. Mitchell JR, Hoeijmakers JH, Niedernhofer LJ. Divide and conquer: nucleotide excision repair battles cancer and ageing. *Curr Opin Cell Biol*. 2003;15:232–240.
16. Lombard DB, Chua KF, Mostoslavsky R, Franco S, Gostissa M, Alt FW. DNA repair, genome stability, and aging. *Cell*. 2005;120:497–512.
17. Chang D, Chen F, Zhang F, McKay B, Ljungman M. Dose-dependent effects of DNA-damaging agents on p53-mediated cell cycle arrest. *Cell Growth Differ*. 1999;10:155–162.
18. Ljungman M, Zhang F, Chen F, Rainbow A, McKay B. Inhibition of RNA polymerase II as a trigger for the p53 response. *Oncogene*. 1999;18:583–592.
19. Ljungman M, Lane DP. Transcription - guarding the genome by sensing DNA damage. *Nat Rev Cancer*. 2004;4:727–737.
20. McKay B, Ljungman M. Role for p53 in the recovery of transcription and protection against apoptosis induced by ultraviolet light. *Neoplasia*. 1999;1:276–284.
21. McKay B, Ljungman M, Rainbow A. Persistent DNA damage induced by ultraviolet light inhibits p21(waf1) and bax expression: implications for DNA repair, UV sensitivity and the induction of apoptosis. *Oncogene*. 1998;17:545–555.
22. McKay B, Chen F, Perumalswami C, Zhang F, Ljungman M. The tumor suppressor p53 can both stimulate and inhibit ultraviolet light-induced apoptosis. *Mol Biol Cell*. 2000;11:2543–2551.
23. Ljungman M, Zhang F. Blockage of RNA polymerase as a possible trigger for ultraviolet light-induced apoptosis. *Oncogene*. 1996;13:823–831.
24. Berardi P, Russell M, El-Osta A, Riabowol K. Functional links between transcription, DNA repair and apoptosis. *Cell Mol Life Sci*. 2004; 61:2173–2180.
25. Scicchitano DA, Olesnicky EC, Dimitri A. Transcription and DNA adducts: what happens when the message gets cut off? *DNA Repair*. 2004;3:1537–1548.
26. Yanamadala S, Ljungman M. Potential role of MLH1 in the induction of p53 and apoptosis by blocking transcription on damaged DNA templates. *Mol Cancer Res*. 2003;1:747–754.
27. Imoto K, Kobayashi N, Katsumi S, et al. The total amount of DNA damage determines ultraviolet-radiation-induced cytotoxicity after uniform or localized irradiation of human cells. *J Invest Dermatol*. 2002;119:1177–1182.
28. Nishiwaki Y, Kobayashi N, Imoto K, et al. Trichothiodystrophy fibroblasts are deficient in the repair of ultraviolet-induced cyclobutane pyrimidine dimers and (6-4)photoproducts. *J Invest Dermatol*. 2004;122:526–532.
29. Mori T, Nakane M, Hattori T, Matsunaga T, Ihara M, Nikaido O. Simultaneous establishment of monoclonal antibodies specific for either cyclobutane pyrimidine dimer or (6-4)photoproduct from the same mouse immunized with ultraviolet-irradiated DNA. *Photochem Photobiol*. 1991;54:225–232.
30. Van Houten B, Cheng S, Chen Y. Measuring gene-specific nucleotide excision repair in human cells using quantitative amplification of long targets from nanogram quantities of DNA. *Mutat Res*. 2000;460:81–94.
31. Ayala-Torres S, Chen Y, Svoboda T, Rosenblatt J, Van Houten B. Analysis of gene-specific DNA damage and repair using quantitative polymerase chain reaction. *Methods*. 2000;22:135–147.
32. Santos JH, Meyer JN, Mandavilli BS, Van Houten B. Quantitative PCR-based measurement of nuclear and mitochondrial DNA damage and repair in mammalian cells. *Methods Mol Biol*. 2006;314:183–199.
33. Ljungman M. Recovery of RNA synthesis from the DHFR gene following UV-irradiation precedes the removal of photolesions from the transcribed strand. *Carcinogenesis*. 1999;20:395–399.
34. Clingen PH, Arlett CF, Cole J, et al. Correlation of UVC and UVB cytotoxicity with the induction of specific photoproducts in T-lymphocytes and fibroblasts from normal human donors. *Photochem Photobiol*. 1995;61:163–170.
35. Masutani C, Sugasawa K, Yanagisawa J, et al. Purification and cloning of a nucleotide excision repair complex involving the xeroderma pigmentosum group C protein and a human homologue of yeast RAD23. *EMBO J*. 1994;13:1831–1843.
36. Batty D, Rapic'-Otrin V, Levine AS, Wood RD. Stable binding of human XPC complex to irradiated DNA confers strong discrimination for damaged sites. *J Mol Biol*. 2000;300:275–290.
37. Sugasawa K, Ng JMY, Masutani C, et al. Xeroderma pigmentosum group C protein complex is the initiator of global genome nucleotide excision repair. *Mol Cell*. 1998;2:223–232.
38. Sugasawa K, Shimizu Y, Iwai S, Hanaoka F. A molecular mechanism for DNA damage recognition by the xeroderma pigmentosum group C protein complex. *DNA Repair*. 2002;1:95–107.
39. Sugasawa K, Okamoto T, Shimizu Y, Masutani C, Iwai S, Hanaoka F. A multistep damage recognition mechanism for global genomic nucleotide excision repair. *Genes Dev*. 2001;15:507–521.
40. Laine JP, Egly JM. When transcription and repair meet: a complex system. *Trends Genet*. 2006;22:430–436.
41. Mellon I. Transcription-coupled repair: a complex affair. *Mutat Res*. 2005;577:155–161.
42. O'Donovan A, Davies AA, Moggs JG, West SC, Wood RD. XPG endonuclease makes the 3′ incision in human DNA nucleotide excision repair. *Nature*. 1994;371:342–345.
43. Enzlin JH, Schärer OD. The active site of the DNA repair endonuclease XPF–ERCC1 forms a highly conserved nuclease motif. *EMBO J*. 2002; 21:2045–2053.
44. Setlow RB. Repair deficient human disorders and cancer. *Nature*. 1978;271:713–717.
45. Suzuki F, Han A, Lankas GR, Utsumi G, Elkind MM. Spectral dependencies of killing, mutation, and transformation in mammalian cells and their relevance to hazards caused by solar ultraviolet radiation. *Cancer Res*. 1981;41:4916–4924.
46. Billecke CA, Ljungman M, McKay B, Rehemetull A, Taneja N, Ethier SP. Lack of functional pRb results in attenuated recovery of mRNA synthesis and increased apoptosis following UV radiation in human breast cancer cells. *Oncogene*. 2002;21:4481–4489.
47. Conforti G, Nardo T, D'Incalci M, Stefanini M. Proneness to UV-induced apoptosis in human fibroblasts defective in transcription coupled repair is associated with the lack of Mdm2 transactivation. *Oncogene*. 2000;19:2714–2720.
48. Therrien JP, Drouin R, Baril C, Drobetsky EA. Human cells compromised for p53 function exhibit defective global and transcription-coupled nucleotide excision repair, whereas cells compromised for pRb function are defective only in global repair. *Proc Natl Acad Sci U S A*. 1999;96:15038–15043.
49. Mullaart E, Roza L, Lohman PHM, Vijg J. The removal of UV-induced pyrimidine dimers from DNA of rat skin cells in vitro and in vivo in relation to aging. *Mech Ageing Dev*. 1989;47:253–264.
50. van der Wees CGC, Vreeswijk MPG, Persoon M, van der Laarse A, van Zeeland AA, Mullenders LHF. Deficient global genome repair of UV-induced cyclobutane pyrimidine dimers in terminally differentiated myocytes and proliferating fibroblasts from the rat heart. *DNA Repair*. 2003;2:1297–1308.
51. Vijg J, Mullaart E, van der Schans GP, Lohman PHM, Knook DL. Kinetics of ultraviolet induced DNA excision repair in rat and human fibroblasts. *Mutat Res*. 1984;132:129–138.
52. Hanawalt PC. Revisiting the rodent repairadox. *Environ Mol Mutagen*. 2001;38:89–96.
53. Leadon SA, Snowden M. Differential repair of DNA damage in the human metallothionein gene family. *Mol Cell Biol*. 1998;8:5331–5338.
54. Sancar A. DNA excision repair. *Ann Rev Biochem*. 1996;65:43–81.
55. Dip R, Camenisch U, Naegeli H. Mechanisms of DNA damage recognition and strand discrimination in human nucleotide excision repair. *DNA Repair*. 2004;3:1409–1423.
56. Uchida A, Sugasawa K, Masutani C, et al. The carboxy-terminal domain of the XPC protein plays a crucial role in nucleotide excision repair through interactions with transcription factor IIH. *DNA Repair*. 2002;1:449–461.
57. You JS, Wang M, Lee SH. Biochemical analysis of the damage recognition process in nucleotide excision repair. *J Biol Chem*. 2003; 278:7476–7485.
58. Reardon JT, Sancar A. Recognition and repair of the cyclobutane thymine dimer, a major cause of skin cancers, by the human excision nuclease. *Genes Dev*. 2003;17:2539–2551.

59. Fousteri M, Vermeulen W, van Zeeland AA, Mullenders LHF. Cockayne syndrome A and B proteins differentially regulate recruitment of chromatin remodeling and repair factors to stalled RNA polymerase II in vivo. *Mol Cell*. 2006;23:471–482.
60. Gorgels TGMF, van der Pluijm I, Brandt RMC, et al. Retinal degeneration and ionizing radiation hypersensitivity in a mouse model for Cockayne syndrome. *Mol Cell Biol*. 2006;27:1433–1441.
61. Henning KA, Li L, Iyer N, et al. The Cockayne syndrome group A gene encodes a WD repeat protein that interacts with CSB protein and a subunit of RNA polymerase II TFIIH. *Cell*. 1995;82:555–564.
62. Sarker AH, Tsutakawa SE, Kostek S, et al. Recognition of RNA polymerase II and transcription bubbles by XPG, CSB, and TFIIH: insights for transcription-coupled repair and Cockayne syndrome. *Mol Cell*. 2005;20:187–198.
63. Groisman R, Kuraoka I, Chevallier O, et al. CSA-dependent degradation of CSB by the ubiquitin-proteasome pathway establishes a link between complementation factors of the Cockayne syndrome. *Genes Dev*. 2006;20:1429–1434.
64. Ikeno Y, Bronson RT, Hubbard GB, Lee S, Bartke A. Delayed occurrence of fatal neoplastic diseases in Ames dwarf mice: correlation to extended longevity. *J Gerontol Biol Sci Med Sci*. 2003;58A: 291–296.
65. van Buul PPW, van Buul-Offers S. Effect of hormone treatment on spontaneous and radiation-induced chromosomal breakage in normal and dwarf mice. *Mutat Res*. 1982;106:237–246.
66. van Buul PPW, van Buul-Offers SC. Effects of hormone treatment on chromosomal radiosensitivity of somatic and germ cells of Snell's dwarf mice. *Mutat Res*. 1988;198:263–268.
67. Bickis I, Estwick RR, Campbell JS. Observations on initiation of skin carcinoma in pituitary dwarf mice. I. *Cancer*. 1956;9:763–767.
68. Bielschowsky F, Bielschowsky M. Carcinogenesis in the pituitary of dwarf mouse. The response to dimethylbenzanthracene applied to the skin. *Br J Cancer*. 1961;15:257–262.
69. Bielschowsky F, Bielschowsky M. Carcinogenesis in the pituitary dwarf mouse. The response to 2-aminofluorene. *Br J Cancer*. 1960; 14:195–199.
70. Rennels EG, Anigstein DM, Anigstein L. A cumulative study of the growth of sarcoma 180 in anterior pituitary dwarf mice. *Tex Rep Biol Med*. 1965;23:776–781.
71. Beranek DT. Distribution of methyl and ethyl adducts following alkylation with monofunctional alkylating agents. *Mutat Res*. 1992; 231:11–30.
72. Bohr VA, Anson RM. DNA damage, mutation and fine structure DNA repair in aging. *Mutat Res*. 1995;338:25–34.
73. Mullaart E, Lohman PHM, Berends F, Vijg J. DNA damage metabolism and aging. *Mutat Res*. 1990;237:182–210.
74. Lambert B, Ringborg U, Skoog L. Age-related decrease of ultraviolet light-induced DNA repair synthesis in human peripheral leukocytes. *Cancer Res*. 1979;39:2792–2795.
75. Gerda Nette E, Xi YP, Sun YK, Andrews AD, King DW. A correlation between aging and DNA repair in human epidermal cells. *Mech Ageing Dev*. 1984;24:283–292.
76. Srivastava VK, Busbee DL. Decreased fidelity of DNA polymerases and decreased DNA excision repair in aging mice: effects of caloric restriction. *Biochem Biophys Res Commun*. 1992;182:712–721.
77. Kempf C, Schmitt M, Danse JM, Kempf J. Correlation of DNA repair synthesis with ageing in mice, evidenced by quantitative autoradiography. *Mech Ageing Dev*. 1984;26:183–194.
78. Hart RW, Setlow RB. Correlation between deoxyribonucleic acid excision-repair and life-span in a number of mammalian species. *Proc Natl Acad Sci U S A*. 1974;71:2169–2173.
79. Francis AA, Lee WH, Regan JD. The relationship of DNA excision repair of ultraviolet-induced lesions to the maximum life span of mammals. *Mech Ageing Dev*. 1981;16:181–189.
80. Treton JA, Courtois Y. Correlation between DNA excision repair and mammalian lifespan in lens epithelial cells. *Cell Bio Int Rep*. 1980; 6:253–260.
81. Harper JM, Salmon AB, Leiser SF, Galecki AT, Miller RA. Skin-derived fibroblasts from long-lived species are resistant to some, but not all, lethal stresses and to the mitochondrial inhibitor rotenone. *Aging Cell*. 2007;6:1–13.
82. Cortopassi GA, Wang E. There is substantial agreement among interspecies estimates of DNA repair activity. *Mech Ageing Dev*. 1996;91:211–218.
83. Weindruch R, Walford RL. *The Retardation of Aging and Disease by Dietary Restriction*. Springfield, IL: C.C. Thomas; 1988.
84. Weraarchakul N, Strong R, Wood WG, Richardson A. The effect of aging and dietary restriction on DNA repair. *Exp Cell Res*. 1989; 181:197–204.
85. Lipman JM, Turturro A, Hart RW. The influence of dietary restriction on DNA repair in rodents: a preliminary study. *Mech Ageing Dev*. 1989;48:135–143.
86. Tilley R, Miller S, Srivastava V, Busbee D. Enhanced unscheduled DNA synthesis by secondary cultures of lung cells established from calorically restricted aged rats. *Mech Ageing Dev*. 1992;63:165–176.
87. Licastro F, Weindruch R, Davis L, Walford R. Effect of dietary restriction upon the age-associated decline of lymphocyte DNA repair activity in mice. *Age*. 1988;11:48–52.
88. Guo Z, Heydari A, Richardson A. Nucleotide excision repair of actively transcribed versus nontranscribed DNA in rat hepatocytes: effect of age and dietary restriction. *Exp Cell Res*. 1998;245:228–238.
89. Patil CK, Mian IS, Campisi J. The thorny path linking cellular senescence to organismal aging. *Mech Ageing Dev*. 2005;126:1040–1045.
90. Cohen HY, Miller C, Bitterman KJ, et al. Calorie restriction promotes mammalian cell survival by inducing the SIRT1 deacetylase. *Science*. 2004;305:390–392.
91. Bauer JH, Helfand SL. New tricks of an old molecule: lifespan regulation by p53. *Aging Cell*. 2006;5:437–440.
92. Narayanan L, Fritzell JA, Baker SM, Liskay RM, Glazer PM. Elevated levels of mutation in multiple tissues of mice deficient in the DNA mismatch repair gene Pms2. *Proc Natl Acad Sci U S A*. 1997;94: 3122–3127.
93. Van Remmen H, Ikeno Y, Hamilton M, et al. Life-long reduction in MnSOD activity results in increased DNA damage and higher incidence of cancer but does not accelerate aging. *Physiol Genomics*. 2003;16:29–37.
94. Andziak B, O'Connor TP, Qi W, et al. High oxidative damage levels in the longest-living rodent, the naked mole-rat. *Aging Cell*. 2006;5: 463–471.
95. Ikeno Y, Bronson RT, Hubbard GB, Lee S, Bartke A. Delayed occurrence of fatal neoplastic diseases in Ames dwarf mice: correlation to extended longevity. *J Gerontol A Biol Sci Med Sci*. 2003;58:291–296.

Received November 7, 2007
Accepted January 7, 2008
Decision Editor: Huber R. Warner, PhD